

Supplementary Information

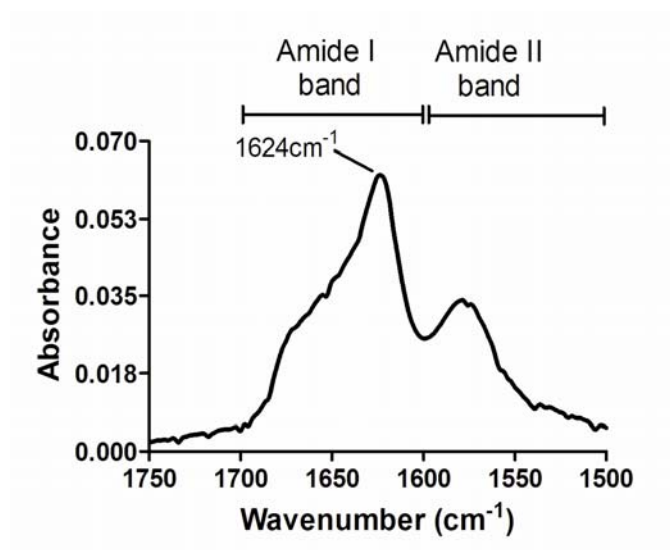
Engineered Nanostructured β -Sheet Peptides Protect Membrane Proteins

Houchao Tao,^{1,5} Sung Chang Lee,^{1,5} Arne Moeller,^{1,2,5} Rituparna Sinha Roy,^{1,4} Fai Yiu Siu,¹ Jörg Zimmermann,³ Raymond C. Stevens,¹ Clinton S. Potter,^{1,2} Bridget Carragher^{1,2} and Qinghai Zhang¹

¹Department of Integrative Structural and Computational Biology, 10550 North Torrey Pines Road, La Jolla, California, USA. ²The National Resource for Automated Molecular Microscopy, 10550 North Torrey Pines Road, La Jolla, California, USA. ³Department of Chemistry, The Scripps Research Institute, 10550 North Torrey Pines Road, La Jolla, California, USA. ⁴Present address: Department of Biological Sciences, Department of Chemical Sciences, Indian Institute of Science Education and Research, Kolkata, India. ⁵These authors contributed equally to this work. Correspondence should be addressed to Q.Z.

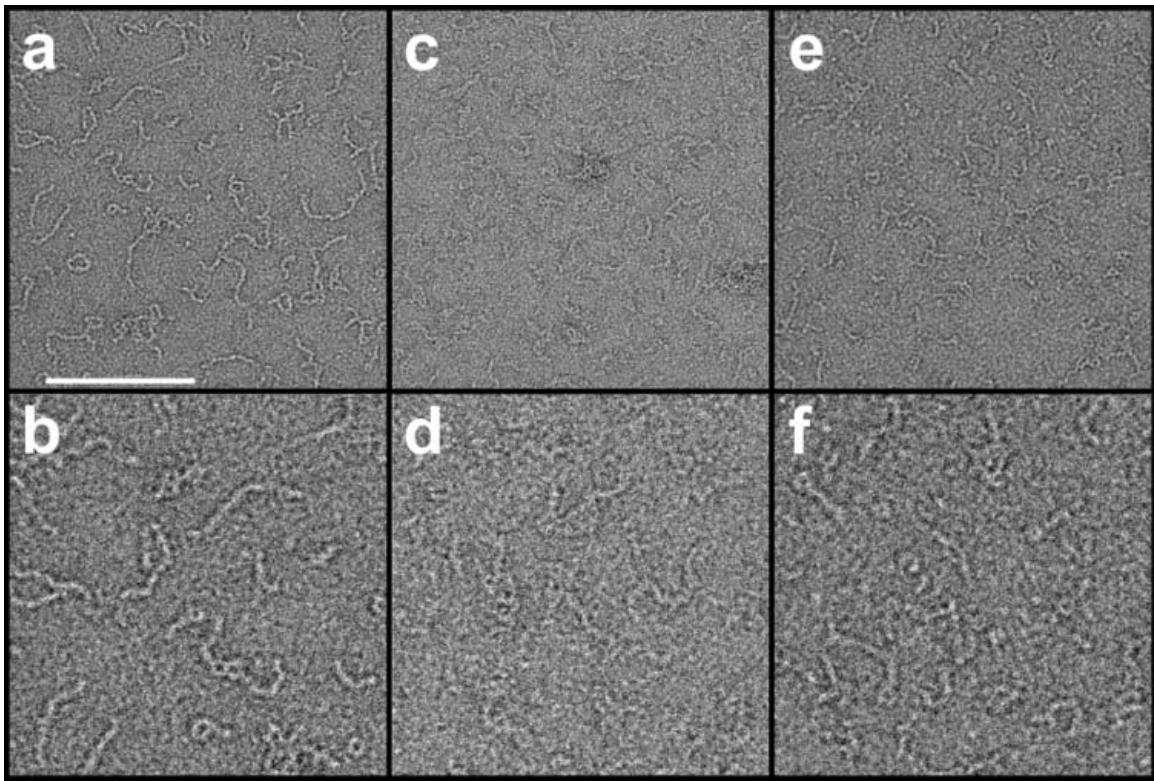
(qinghai@scripps.edu)

Supplementary Figures	Title
Supplementary Figure 1	Fourier transform infrared (FTIR) spectrum of BP-1
Supplementary Figure 2	EM images of designed peptides preserved in negative stain
Supplementary Figure 3	Negative stain EM of BP-1 at gradually decreased concentrations
Supplementary Figure 4	ATPase activity of MsbA in BP-1, SP1D1/dimyristoylphosphatidylcholine nanodiscs, or UDM
Supplementary Figure 5	Stability of bR in BPs
Supplementary Figure 6	Stability of KcsA in BP-1 compared to in detergents and lipid nanodiscs
Supplementary Figure 7	Stability of wild-type GLR monitored by CPM fluorescence thermal denaturation assay
Supplementary Figure 8	EM images of MsbA during dialysis
Supplementary Figure 9	CD characterization of BP-1 in the MsbA sample
Supplementary Figure 10	Random conical tilt pairs of MsbA in BP-1 preserved in negative stain
Supplementary Figure 11	Random conical tilt reconstructions of three MsbA conformations and according fourier shell correlation (FSC) curves
Supplementary Figure 12	Negative staining EM images and ATPase activity of MsbA solubilized in novel amphiphiles

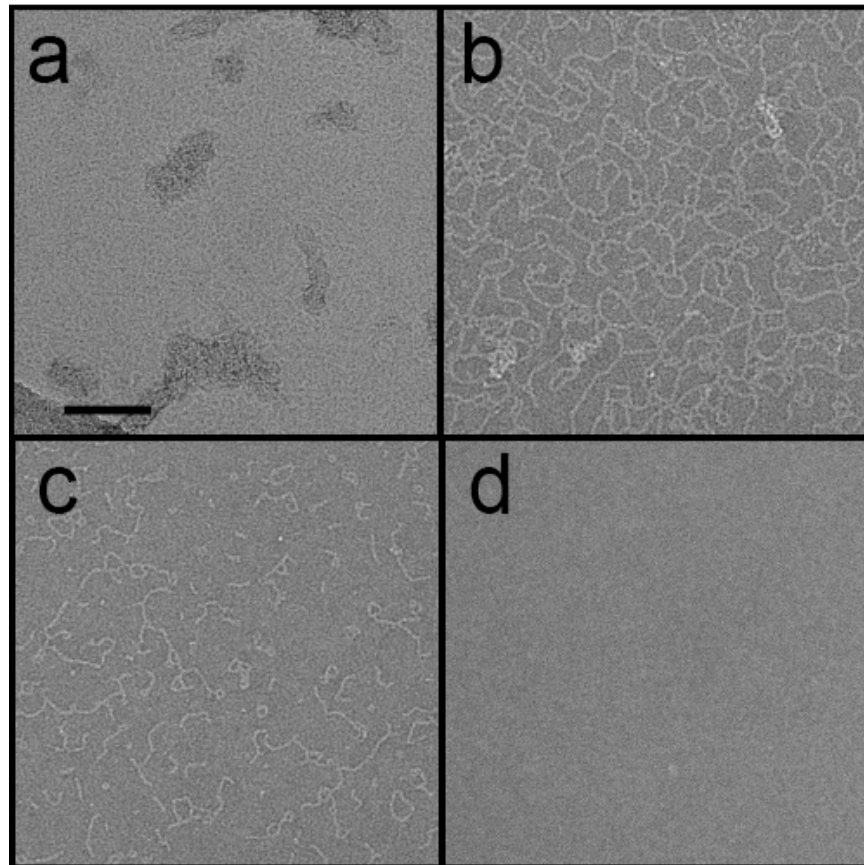


Supplementary Figure 1. Fourier transform infrared (FTIR) spectrum of BP-1. The presence of a major peak (1624 cm⁻¹) in the amide I band (1700 – 1600 cm⁻¹) of BP-1 indicated the formation of β -sheet secondary structures¹.

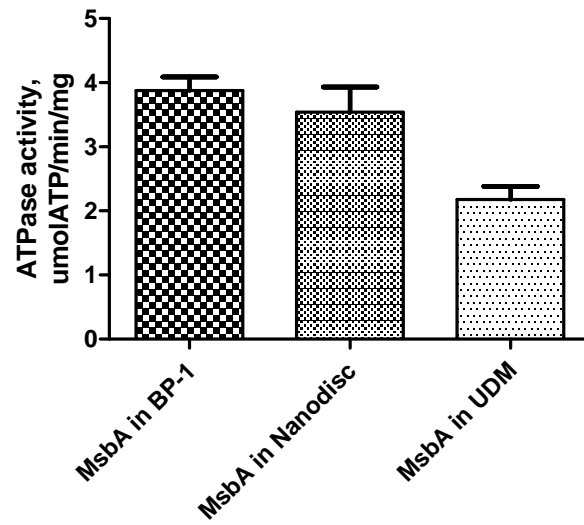
- 1 Adochitei, A. & Drochioiu, G. Rapid Characterization of Peptide Secondary Structure by FT-IR Spectroscopy. *Rev. Roum. Chim.* **56**, 783-791 (2011).



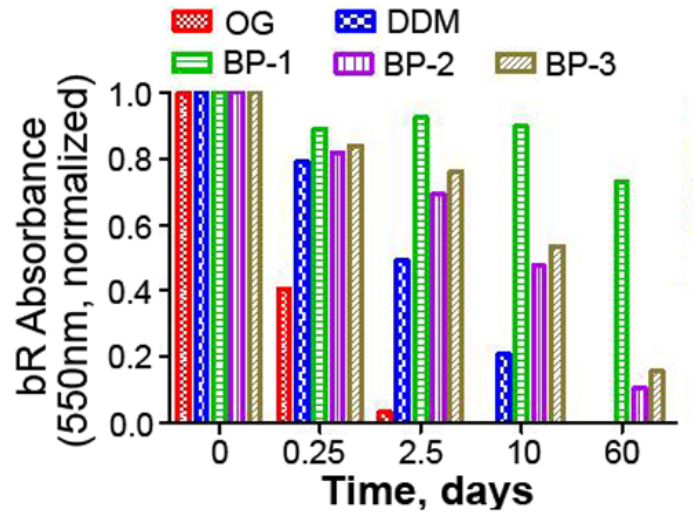
Supplementary Figure 2. EM images of designed peptides preserved in negative stain. **(a-b)** BP-1, **(c-d)** BP-2, **(e-f)** BP-3. Scale bar in upper panel represents 100 nm, and images in lower panels are shown at twofold magnification relative to upper panels.



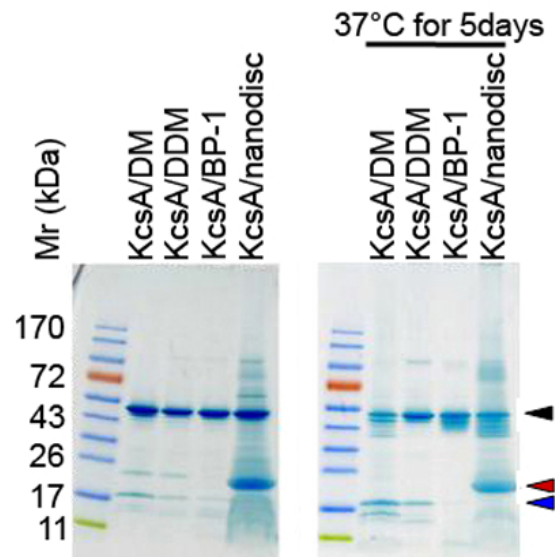
Supplementary Figure 3. Negative stain EM of BP-1 at gradually decreased concentrations. **(a)** BP-1 at 2.5 mM. The filaments cover the entire carbon surface of the grid in multiple layers and significant clustering is visible. Upon dilution **(b)**, 1 to 10; **(c)**, 1 to 100) the number of filaments and clustering gradually decreases as they evenly spread out on the carbon grid. The control with BP1-free buffer **(d)** does not show any of the described filaments but a clean carbon background. Scale bar represents 50nm.



Supplementary Figure 4. ATPase activity of MsbA in BP-1, SP1D1/dimyristoylphosphatidylcholine nanodiscs, or UDM. Data represent an average of >10 measurements from different preparations with means \pm standard error shown.

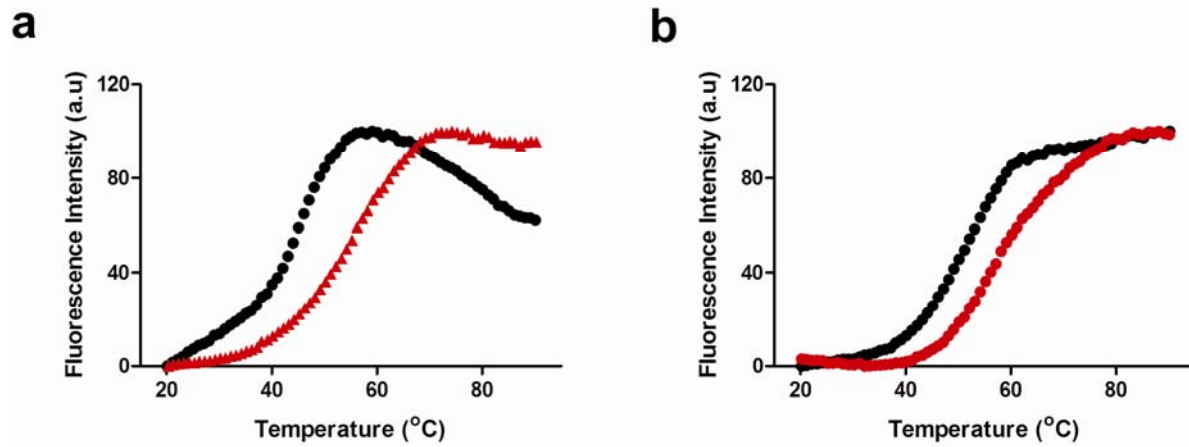


Supplementary Figure 5. Stability of bR in BPs. bR stability in β -D-octylglucoside (OG), β -D-dodecylmaltoside (DDM) or BPs in pH 7.4 buffer (100 mM Tris, 40 mM NaCl) at 37 °C. After first recording characteristic bR absorption spectra, A_{550} was measured periodically; normalized values are plotted.

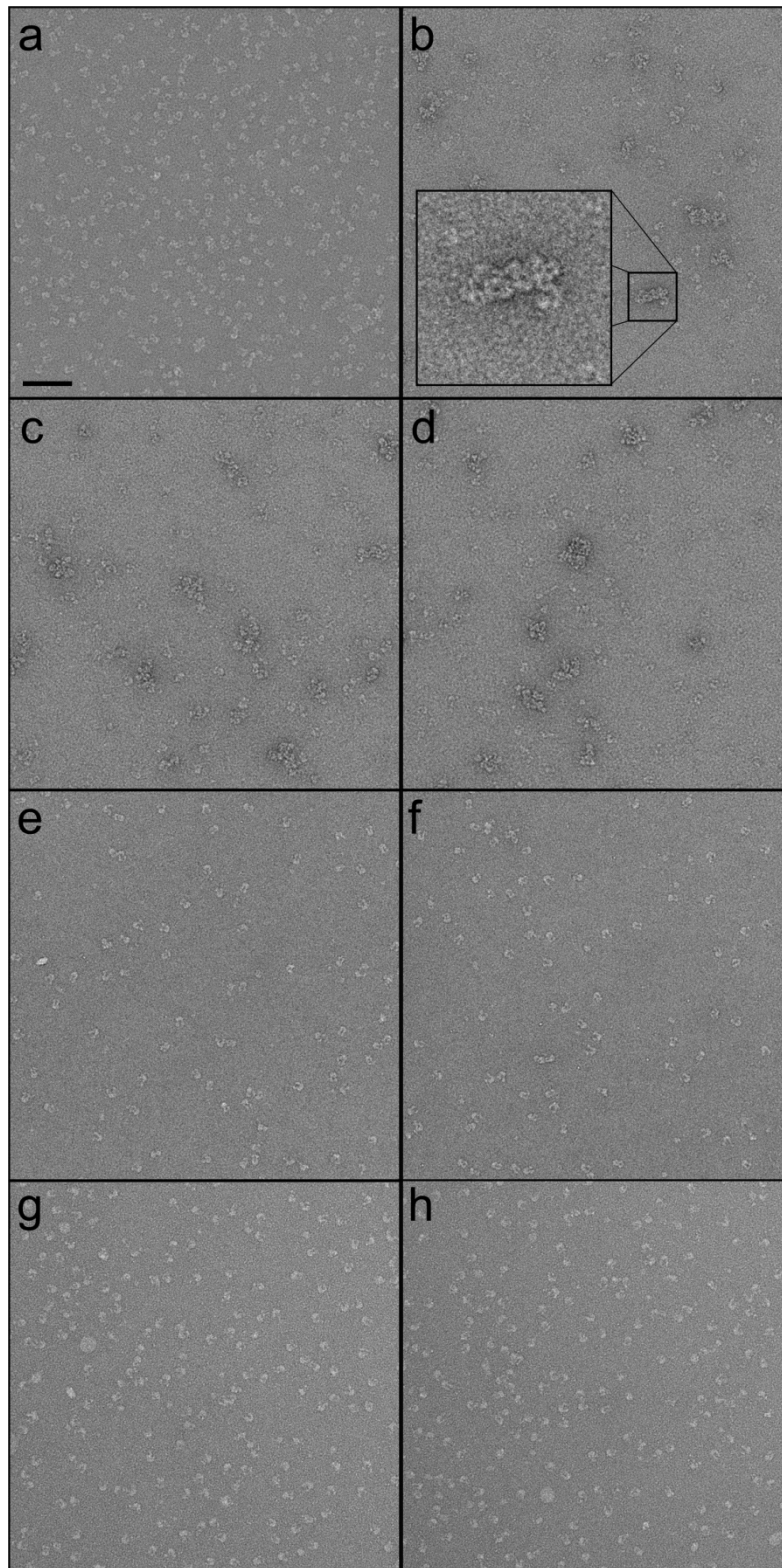


Supplementary Figure 6. Stability of KcsA in BP-1 compared to in detergents and lipid nanodiscs. SDS-PAGE gels show KcsA species before (left) and after 5 days incubation at 37°C (right) in β -D-decylmaltoside (DM), DDM, BP-1 or MSP1D1/dimyristoylphosphatidylcholine nanodiscs. KcsA in BP-1 or nanodiscs showed less monomer appearance than in detergents. Arrows denote KcsA tetramer (~54 kDa), KcsA monomer (~18 kDa), and MSP1D1 (~22 kDa). Bands underneath the major tetramer band represent C-terminal proteolysis products².

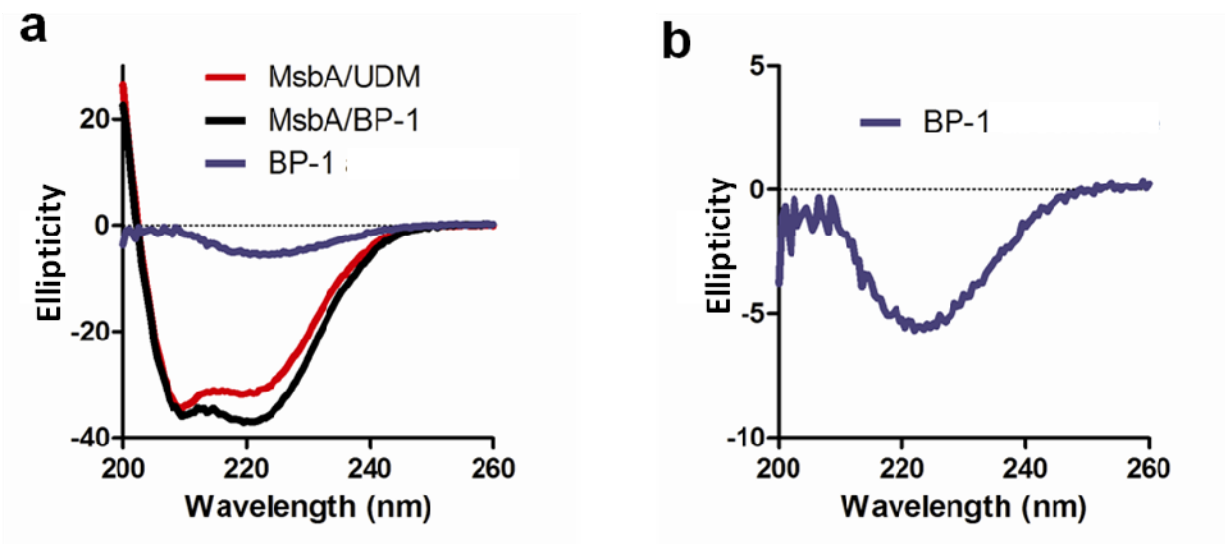
- 2 Cortes, D. M. & Perozo, E. Structural dynamics of the *Streptomyces lividans* K⁺ channel (SKC1): oligomeric stoichiometry and stability. *Biochemistry* **36**, 10343-10352 (1997).



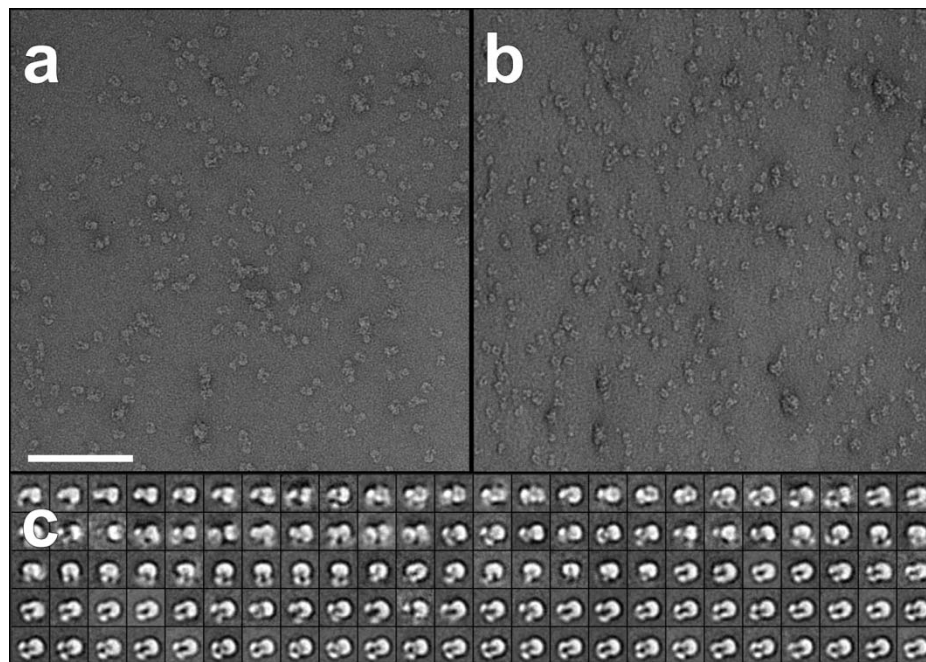
Supplementary Figure 7. Stability of wild-type GLR monitored by CPM fluorescence thermal denaturation assay. **(a)** GLR purified in DDM/CHS was diluted 20-fold into the same buffer containing DDM (0.84 mM) or BP-1 (0.50 mM). Thermal transition temperatures (T_m) were measured as 43.5 ± 0.4 °C and 55.4 ± 1.6 °C for GLR/DDM (black) and GLR/BP-1 (red), respectively. **(b)** GLR/BP-1 sample was prepared by dialysis from the UDM/CHS preparation. T_m values for the GLR sample before (black) and after (red) dialysis were 50.8 ± 0.1 °C and 57.0 ± 2.4 °C, respectively.



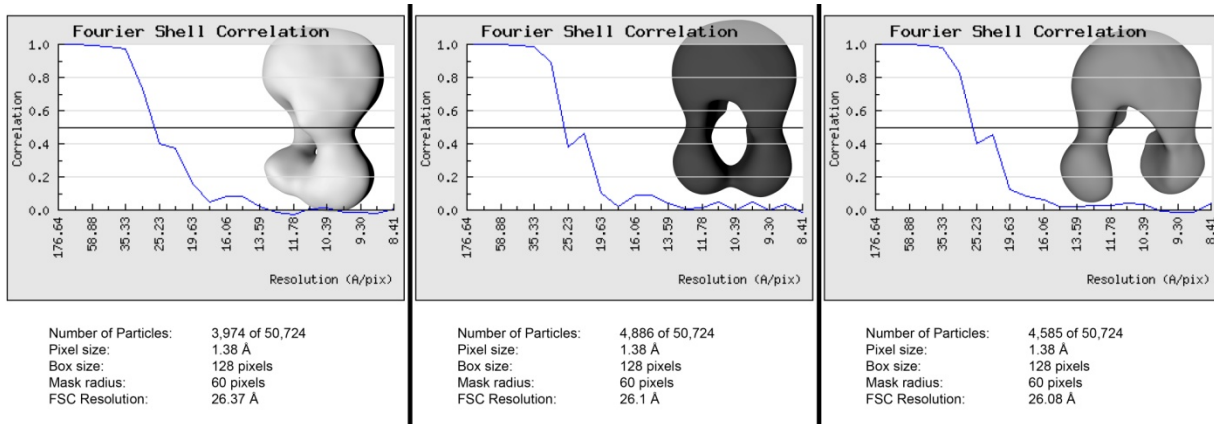
Supplementary Figure 8. EM images of MsbA during dialysis. **(a)** BP-1 preserved MsbA after 48h of dialysis compared to **(b-d)** MsbA in UDM prior to dialysis. While individual MsbA particles are identifiable in UDM the majority are in clusters (see inset in **b**) along with high detergent background. After 30 min of dialysis **(e-f)** the number of isolated particles is enhanced and the clustering is reduced. After 360 min **(g-h)** the particle count is increased, likely due to further reduced clustering or enhanced staining of MsbA/BP-1. Scale bar represents 50nm.



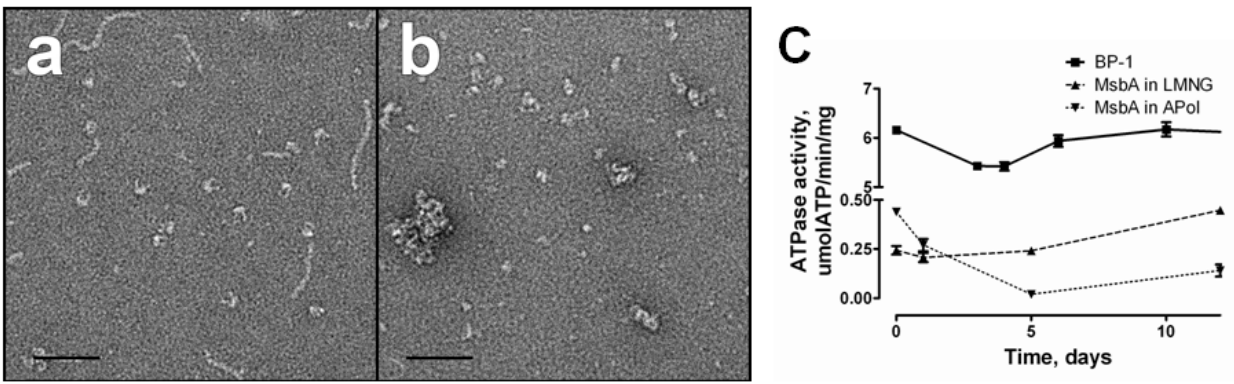
Supplementary Figure 9. CD characterization of BP-1 in the MsbA sample. **(a)** CD spectra of MsbA/UDM (red) and MsbA/BP-1 (black, BP-1 : MsbA ~ 30 : 1 molar ratio). Ellipticity difference (blue) between the two samples, wherein the concentration of MsbA is the same (0.2 mg/mL), is contributed by BP-1. Little background signal from UDM and buffers was corrected. **(b)** Zoom-in on the BP-1 spectrum in **(a)**.



Supplementary Figure 10. Random conical tilt pairs of MsbA in BP-1 preserved in negative stain. **(a-b)** corresponding tilt pairs at 0° and -55° stage tilt. Scale bar represents 100 nm. **(c)** 120 class averages, generated from automatically selected particles using reference free procedures, show multiple MsbA conformers with the two NBDs separated at varied distances.



Supplementary Figure 11. Random conical tilt reconstructions of three MsbA conformations and according fourier shell correlation (FSC) curves. The FSC resolution (0.5) and particle numbers used for the reconstitution are listed.



Supplementary Figure 12. Negative staining EM images and ATPase activity of MsbA solubilized in novel amphiphiles. **(a)** Representative EM images of MsbA purified in lauryl maltose neopentyl glycol (LMNG). String-like LMNG detergent background objects were observed, along with well-stained MsbA particles. **(b)** Representative EM images of MsbA reconstituted in Amphipol A8-35. Significant aggregation was evident, and MsbA structural details were difficult to discern. **(c)** MsbA was stable in LMNG over 12 days of incubation at RT, but less stable in Amphipol A8-35, based on periodic ATPase activity measurement. Additionally, relatively low MsbA ATPase activity was detected in LMNG or Amphipol A8-35 compared to BP-1.